Published in final edited form as:
J Med Chem. 2012 June 28; 55(12): 5933–5941. doi:10.1021/jm300489v.

Structural and enzymatic analyses reveal the binding mode of a novel series of *Francisella tularensis* enoyl reductase (FabI) inhibitors

Shahila Mehboob[*], **Kirk E Hevener**, **Kent Truong**, **Teuta Boci**, **Bernard D Santarsiero**[*], and **Michael E Johnson**[*]
Center for Pharmaceutical Biotechnology, University of Illinois at Chicago, 900 S. Ashland Ave., Chicago, IL 60607-7173 (USA)

Abstract

Due to structural and mechanistic differences between eukaryotic and prokaryotic fatty acid synthesis enzymes, the bacterial pathway, FAS-II, is an attractive target for the design of antimicrobial agents. We have previously reported the identification of a novel series of benzimidazole compounds with particularly good antibacterial effect against *Francisella tularensis*, a Category A biowarfare pathogen. Herein we report the crystal structure of the *F. tularensis* FabI enzyme in complex with our most active benzimidazole compound bound with NADH. The structure reveals that the benzimidazole compounds bind to the substrate site in a unique conformation that is distinct from the binding motif of other known FabI inhibitors. Detailed inhibition kinetics have confirmed that the compounds possess a novel inhibitory mechanism that is unique among known FabI inhibitors. These studies could have a strong impact on future antimicrobial design efforts and may reveal new avenues for the design of FAS-II active antibacterial compounds.

INTRODUCTION

Although antimicrobial drug resistance is on the rise globally, there are 1few drug candidates in the discovery pipeline with novel mechanisms offering a significant improvement over current antimicrobial therapies.[1] The situation has become so urgent that the World Health Organization has declared antimicrobial resistance to be one of the three most important threats to human health. There is, therefore, an urgent need for the characterization of novel antimicrobial targets and the discovery of new mechanisms of antimicrobial action. One particularly attractive antimicrobial drug target is the bacterial fatty acid synthesis pathway (FAS-II), which has seen some attention in recent years.[2] In bacteria, fatty acid synthesis is carried out by a series of discrete enzymes, whereas in mammals it takes place on a single, multi-enzyme complex known as FAS-I. The FAS-I complex and the FAS-II enzymes are structurally and mechanistically distinct, which strongly implies the possibility of selective antimicrobial targeting of bacterial pathogens. The NADH-dependent enzyme, enoyl-ACP reductase I (FabI), catalyzes a rate-limiting step in the FAS-II elongation cycle, and is one of the more appealing target enzymes in this pathway.[3] The FabI enzyme is a member of the short-chain alcohol dehydrogenase / reductase (SDR) superfamily characterized by a catalytic triad of key tyrosine, lysine, and serine residues that reduce a key double bond in the enoyl substrate.[4]

[*]Corresponding Authors: Shahila Mehboob, phone: 312-413-9304, shahila@uic.edu; Bernard D Santarsiero, phone: 312-413-0339, bds@uic.edu; Michael E Johnson, phone: 312-996-9114, mjohnson@uic.edu.

Though once suggested to be a potential target for the development of broad-spectrum inhibitors, FabI has recently been shown to be one of several enoyl reductase isozymes, including FabK, FabL and FabV, that can be present in addition to or in place of FabI, depending on the bacterial species.[5–8] For example, the enterococci and streptococci solely express FabK, which has no sequence or structural similarity to FabI and reduces the enoyl substrate by a separate mechanism.[9] Similarly FabL and FabV, which are structurally and mechanistically similar to FabI, but resistant to known FabI inhibitors, are present alongside FabI in *B. subtilis* and *P. aeruginosa*, respectively. The presence of enoyl reductase isozymes in these and other species bypass the effect of any known inhibitor of FabI. However, several Gram-negative organisms, including *F. tularensis*, *E. coli* and *H. pylori*, express only the FabI isozyme, suggesting essentiality in these species. Further evidence of target essentiality in *F. tularensis* has been provided by Lu *et al.*, who showed a strong positive linear correlation between K_i, and MIC values for their diphenyl ether FabI inhibitors, which strongly suggested that FabI is the primary cellular target for these compounds.[10] The most compelling evidence so far demonstrating *in vivo* essentiality is the ability of these compounds to rescue animals in a *F. tularensis* infection model in mice.[10,11]

Recently, there has been vigorous debate concerning the essentiality of the FAS-II pathway in Gram-positive organisms with respect to their ability to uptake required fatty acids from the host environment.[12–14] It has now been shown that some Gram-positive species, including the streptococci, possess a feedback regulatory system that can suppress the endogenous pathway when exogenous fatty acids are present, while other species, such as *S. aureus* are not able to do so and remain susceptible to FAS-II inhibition.[15] However, the susceptibility of Gram-negative organisms, such as *F. tularensis*, to FAS-II inhibition has not been questioned. This is because they require β-hydroxy-fatty acids to assemble the lipid A component of outer membrane lipopolysaccharides. Exogenous fatty acids from mammalian hosts cannot support lipid A synthesis because the bacteria have no mechanism to transfer the acyl chains from CoA to the acyl carrier protein (ACP) of FAS-II such that the hydroxyl group can be introduced.[16]

Francisella tularensis and the need for new antibacterial compounds

Francisella tularensis is the causative agent of the zoonosis, tularemia, which has an average of only 125 case reports per year in the United States.[17] However, the organism is easily aerosolized, has a high mortality rate of up to 30% and has a low infectious dose of as few as 10 cells.[17] Because of this, the United States federal government has classified *F. tularensis* as a Category A priority pathogen posing high risk to national security and public health. The current treatment standard for tularemic infection is a regimen containing an aminoglycoside (streptomycin or gentamicin) or a tetracycline as second-line option, with doxycycline most commonly recommended.[18] Unfortunately, the requirement for intravenous administration of the aminoglycosides and the contraindication of tetracyclines in pregnant women and children make these medicines less than ideal choices in the event of a mass casualty situation. There is, therefore, significant interest in the development of alternative therapies for the treatment of tularemia.

A surprisingly diverse range of compounds with unique scaffolds have been reported as inhibitors of bacterial enoyl-ACP reductase type I enzymes. These include the diazaborines and isoniazid, which inhibit the enzyme by covalent attachment; diphenyl ethers, aminopyridines, indole naphthyridinones, indole piperazines, thiopyridines, 4-pyridones, and pyrazoles.[2] Among these, only isoniazid, an antitubercular agent, and the diphenyl ether, triclosan, have seen commercial usage. Triclosan has been of particular interest, due to its broad spectrum of activity against a number of both Gram-positive and Gram-negative organisms, and is currently considered the prototypical FabI inhibitor.[19,20] Because of this, the diphenyl ether scaffold has received considerable attention in the antibacterial drug

discovery arena.[21–27] Unfortunately, the diphenyl scaffold has significant disadvantages, including high serum binding and metabolic inactivation through glucuronidation and sulfation. The remaining scaffolds mentioned above also have significant hurdles which have limited their clinical utility to date. The use of diazaborines is associated with toxicity concerns,[28] while the aminopyridines, indole naphthyridinones, thiopyridines, and 4-pyridones have a narrow spectrum of antimicrobial activity exhibiting activity against *S. aureus*, *E. coli* and *B. subtilis*.[29–31]

Although chemically diverse, the known inhibitors of the FabI enzyme have several features in common which contribute to their inhibitory mechanisms. The first is an aromatic or delocalized planar moiety that can participate in π-stacking interactions. This group is observed in nearly all published structures to engage the aromatic nicotinamide ring of NAD^+, the cofactor product of the FabI reaction. The second is a hydrogen bond accepting group that can interact with an active site tyrosine residue. Figure 1 shows the structures of the known FabI inhibitors discussed above with the key binding functionalities highlighted. Another important feature of FabI inhibition is the slow-inhibition seen with several published inhibitors that has been explained to be due to the ordering of a key flexible loop region upon inhibitor binding.[10] Taken together, these features describe the known pattern of inhibition that has been seen to date.

Recently we have reported a novel series of inhibitors based on a benzimidazole scaffold possessing enzyme inhibitory activity equipotent to that of triclosan.[32] The inhibitors showed promising activity against both Gram-positive and Gram-negative organisms in whole-cell antimicrobial tests and represented a unique chemical class that had not been previously reported. Herein, we report the solution of a co-crystal structure of FabI from *F. tularensis* bound to the most active inhibitor, Compound **1** (ChemBridge ID 7725253), which has an IC_{50} of 0.3 μM. The ternary complex, which includes the NADH cofactor, shows the key binding interactions between Compound **1** and NADH with the FabI active site residues and reveals that the benzimidazole compounds inhibit FabI by binding to the active site in a manner that differs significantly from the known inhibitory patterns seen to date. Enzyme inhibition kinetics experiments performed using compounds from this class confirm the unique binding motif, as will be discussed below.

METHODS

Protein Expression and Purification

The gene for FabI (from *F. tularensis* subsp. *tularensis* Schu4) was commercially synthesized (Bio Basic Inc., Canada) after codon optimization. The gene was ligated into a pET-15b vector with an N-terminal His tag and transformed into *Escherichia coli* BL21 (DE3) cells. The cells were grown at 310 K and induced with 1 m*M* IPTG when the OD reached 0.5. The cells were harvested after an additional 4 h of growth. Sonication was used to lyse the cells and the supernatant was loaded onto a nickel-chelated His-Trap column (GE Healthcare) and eluted with a stepwise gradient of imidazole in 50 m*M* Tris, 500 m*M* NaCl pH 8.0. The final purification step used a size-exclusion column (Superdex-200 26/60 from GE Healthcare) previously equilibrated with buffer consisting of 50 m*M* Tris, 100 m*M* NaCl pH 8.0 with 1 m*M* DTT. The FabI enzyme was soluble when over-expressed, and was purified to >98% purity.

Crystallization and Data Collection

Initial screening for crystallization conditions of Compound 1 bound to FtuFabI was carried out using a 96-well plate and a Mosquito robotic system using the facilities at Argonne National Laboratory. The microcrystals obtained were further optimized using hanging-drop

methods. For the ternary FtuFabI-NADH-Compound 1 complex, FtuFabI at a concentration of 18mg/ml was incubated with 1mM NADH and 1mM Compound 1 for 1 hr at room temperature prior to crystallization set up. Diffraction quality crystals were obtained with the buffer containing 0.1M sodium acetate pH4.6 and 2.25M ammonium sulfate. Crystals were cryoprotected with 10% glycerol and data were collected from one crystal on the SER-CAT 22-ID beamline at the Advanced Photon Source, Argonne National Laboratory using a wavelength of 1 Å, a sample-to-detector distance of 320 mm and an oscillation angle of 1°. A complete dataset was recorded on a MAR-CCD 300 to a resolution of 2.25 Å. Diffraction data were processed and scaled using XDS.[33] The crystal belonged to space group $P2_1$ and contained 16 chains in the asymmetric unit. The unit cell parameters and data collection statistics are shown in Table 1.

Structure Solution and Refinement

The structure of FtuFabI (with NADH and Compound 1) was solved by molecular replacement using Phaser [34] in the CCP4 program suite (Collaborative Computational Project 1994) and the coordinates of FtuFabI complexed with NAD^+ and triclosan (PDB ID 3NRC). [35] Refinement was carried out using Refmac5.5.[36] Refinement included data in the range of 20 – 2.5 Å. A total of 5% of the data were omitted from refinement for R_{free} calculations. The model was built using the program COOT.[37] After a few cycles of restrained refinement, positive features in the electron density map were assigned as atoms of NADH and placed. Compound 1 was then fit into the remaining positive electron density found in the active site. The final refinement statistics together with the statistics concerning the geometry of the final models are given in Table 1. The final model has an R_{cryst} of 24.1% and R_{free} of 29.2%. The model was validated using Molprobity.38 The majority of the residues lie in the most favored regions of the Ramachandran plot and the remainder are in the generously allowed regions. The coordinates of the structure of FtuFabI complexed with NADH and Compound 1 have been deposited in the PDB under accession code 3UIC.

Enzymatic Assay

The FabI reaction converts one molecule of NADH and crotonyl-CoA into NAD^+ and butyryl-CoA. Details of the assay have been presented elsewhere.[32] Enzyme activity was recorded by following the rate of decrease in fluorescence of NADH at 460nm (excitation wavelength 340nm). Inhibition kinetics were performed by varying the concentration of Compound 1 and one substrate (NADH or crotonyl-CoA) while keeping the other substrate at a constant concentration. The experimental data were fit to eqs 1–3 by nonlinear regression analysis in SigmaPlot11.0 with Enzyme Kinetics Module 1.3. The kinetic mechanism and relevant kinetic parameters were derived from the best fit to eq. 1 for competitive inhibition, eq. 2 for uncompetitive inhibition, eq. 3 for noncompetitive inhibition and eq. 4 for mixed type inhibition.

$$v = V_{max}/(1+K_m/[S])\,(1+[I]/K_i)) \quad \text{for competitive inhibition} \tag{1}$$

$$v = V_{max}/(1+[I]/K_i+K_m/[S]) \quad \text{for uncompetitive inhibition} \tag{2}$$

$$v = V_{max}/((1+[I]/K_i)\,(1+K_m/[S])) \quad \text{for non competitive inhibition} \tag{3}$$

$$v = V_{max}/(K_m/[S])\,(1+[I]/K_i)+1+[I]/\alpha K_i) \quad \text{for mixed-type inhibition} \tag{4}$$

where v is the reaction rate (which in our case is the rate of change of relative fluorescence intensity), V_{max} is the maximum rate of the reaction, [S] is the substrate concentration (μM), [I] is the inhibitor concentration (μM), K_m is the Michaelis-Menten constant for substrate S, K_i is the dissociation constant of the inhibitor I to the free enzyme and αK_i is the dissociation constant for the inhibitor I to the ES complex.

RESULTS AND DISCUSSION

Structural Analysis of the Benzimidazole Binding Interactions

The crystal structure of FtuFabI in complex with Compound 1 (Figure 2) was solved in the $P2_1$ space group to a resolution of 2.5 Å using the molecular replacement method with a single chain from the crystal structure of FtuFabI in complex with triclosan (PDB ID 3NRC).[35] The asymmetric unit contains 16 chains with four tetramers stacked up on one another along the a-axis direction (Figure 2A). We have previously shown, using dynamic light scattering and size exclusion studies, that FtuFabI is a tetramer at concentrations above 60 μM.[35] In these crystallization experiments FtuFabI is predominantly tetrameric, however we were unable to refine the structure in the $P2_12_12$ space group, as we previously did with FtuFabI-triclosan complex structure[35] so small displacements at the tetramer-tetramer interface must reduce the overall crystallographic Laue group symmetry from Pmmm to P2/m. Both NADH and Compound 1 (Figure 2B) are present in each of the 16 chains. Although it is not possible to determine at this resolution whether NADH or NAD^+ is present in the active site, our use of NADH over NAD^+ in the crystallization procedure, as well as the absence of any substrate, strongly suggests that the reduced form, NADH, is the species present. The structures of the different chains were restrained to be identical during refinement. We focus on the features of chain A in our discussions henceforth since it is representative of each of the chains.

Compound 1 binds to FtuFabI in the substrate binding region, the same region to which triclosan binds (Figure 3). Importantly, unlike triclosan and other known inhibitors, we do not observe π-stacking of either the benzimidazole ring system or the phenyl ring of Compound 1 against the nicotinamide ring of NADH. This observation is supported by binding kinetics experiments discussed below and is also addressed in the following SAR analysis section. The N_3 atom of the benzimidazole ring system occupies the same location as the phenolic hydroxyl group of triclosan placing it in a position in which it can engage either the hydroxyl group of Tyr156 or the 2'-ribose hydroxyl group of the NADH cofactor forming a hydrogen bond in a manner similar to triclosan (Figure 4A). The chlorine atoms on the phenyl ring of Compound 1 are positioned such that the para –Cl atom is 3.5Å away from the backbone carbonyl of Pro154 while the meta chlorine atom points into the hydrophobic pocket created by Leu99 and Ile200 (Figure 4B). The two methyls on the benzimidazole ring point toward the entrance of the active site which is lined by Phe93, Ala94 and Leu99.

The loop element (Gly190- Phe203) is typically disordered or flexible in reported structures of the apo-enzyme or binary complexes with only the cofactor. This loop adopts a closed conformation in our structure, forming van der Waals interactions with Compound 1 and hydrogen bonds with the NADH cofactor. A small α-helix turn develops in the flexible loop upon substrate binding, and has been noted in previous co-crystal structures with bound inhibitors.[35] The loop's hydrophobic residues Ala196, Ala197, Ile200, Phe203 face internally toward Compound 1, and contribute to the steric fit of the compound in the binding site; while Ser198, Ser201 and Asn202 are solvent exposed with Gly199 located at the N-terminal of the α-helix. The NADH cofactor forms a total of 10 hydrogen bonds with the protein, of which four are with residues in this loop element. These include the pyrophosphate groups of NADH which interact with Thr194 (2.8 Å), the backbone of

Ala196 (3.1 Å), and the carboxamide moiety of the nicotinamide ring which engages the backbone amide of Ile192 (2.9 Å and 3.0 Å). The interactions between residues in this loop and both the inhibitor and cofactor appear critical to the binding and activity of Compound 1 (Figure 5). Interestingly, portions of this mobile loop element, along with a series of basic residues immediately adjacent have been proposed to be involved in recognition and binding of the acyl-carrier protein of the natural substrate, which would place it in a position significantly different from that seen in this and other structures with inhibitors bound.[39] The ordering of this loop upon inhibitor binding and its role in the slow-binding effects seen with some inhibitors of the FabI enzyme has previously been discussed.[10]

One of the most conserved features observed in published FabI inhibitors to date is the presence of a hydrogen bond acceptor on the ligand at a position that can engage in hydrogen bonding with the hydroxyl of Tyr156 and/or the 2'-hydroxyl of the nicotinamide ribose of the nucleotide cofactor (Figure 4A). In the case of the indole naphthyridinones[29] and aminopyridine[40] based inhibitors the amide carbonyl acts as the key acceptor (PDB IDs 1MFP, 3OIG, 3OJF and 1LXC) (Figure 1). Similar interaction patterns are observed in other published classes of inhibitors.[41] In contrast, triclosan has two functional groups, the phenolic hydroxyl group and the diphenyl ether, which have been proposed to be involved in this key interaction, thereby increasing the binding affinity of triclosan for the FabI enzyme. (PDB IDs 2QIO and 3NRC).[27,35,42] There is, however, some uncertainty regarding the propensity of the diphenyl ether group to form hydrogen bonds in general, which has been discussed, though the significantly greater activity of triclosan over other known classes is well documented.[43]

Application of Structural Analysis to Known Benzimidazole SAR

The X-ray crystal structure indicates that the benzimidazole compound forms a stable ternary complex with FtuFabI. This complex is observed in the active site of all chains in the solved structure. We have previously presented a preliminary structure-activity analysis developed using a number of analogs of Compound 1, which we can now support and expand upon using the observed binding conformation in this structure.[32] We found that substituting the methylene linker between the benzimidazole ring system and the phenyl ring with a methanone group at position 8 (Figure 6) results in a complete loss of activity. We believe this is due to a significant disruption in the geometry of the compound as the sp^3 group is modified to sp^2 hybridization. The resulting change of conformation to a structure that is more planar in character yields a compound that is unable to bind in the non-planar binding conformation that is observed in this structure. Interestingly, the motif of two aromatic groups separated by a small sp^3 linking group that is seen in the diphenyl ether class of inhibitors, such as triclosan, is maintained in the benzimidazole class. However, in the case of the benzimidazole series, the larger, dimethyl-substituted benzimidazole ring system is significantly displaced from the position of the corresponding A-ring in triclosan, which engages in an aromatic stacking interaction with the nicotinamide ring of the NAD^+ cofactor. The larger bulk of the benzimidazole ring system presumably precludes this interaction in the benzimidazole compounds and, as a consequence thereof, also permits the substitution of the methylene linker for the ether linkage, which as mentioned above, has been proposed to also facilitate binding by hydrogen bond interactions.

The phenyl ring of Compound 1 occupies a unique position facing opposite to that seen in the triclosan structure. Unlike triclosan, where the B-ring is facing toward the solvent exposed region, in the benzimidazole compounds the phenyl ring occupies a deeper pocket that is not accessed by triclosan. This pocket is enclosed by the lipophilic groups Ile200, Met206, Phe203 and the rings of Tyr146 and Tyr156. Edge-to-face stacking interactions between Phe203, Tyr156 and the phenyl ring of the benzimidazole compound appear to stabilize the ring in this position and facilitate binding. This positional flip allows the N_3

acceptor on the benzimidazole ring to maintain the key interaction with Tyr156 mentioned above, even though the aromatic stacking interaction is not maintained. It is tempting to speculate that the stabilization of the phenyl ring in this hydrophobic pocket, as well as contributions of direct substituents discussed below, offsets any possible decrease in binding affinity caused by loss of the NAD^+ stacking interaction.

The presence of two chlorine atoms on the phenyl ring, at least one of which (para-Cl) seems to be involved in a halogen bond, contributes significantly to the binding affinity of Compound 1 for the enzyme. Halogen bonds in ligand-target complexes are now recognized as a kind of intermolecular interaction that favorably contribute to the stability of protein-ligand complexes.[44] Halogen bonds are significantly weaker than hydrogen bonds but play a unique role in many complexes including the FabI-triclosan complex. In the benzimidazole structure, the importance of a para-substituted chlorine or bromine atom was a key observation in the reported SAR, however the site of the exact interaction was uncertain. The solved structure shows that the para-chlorine atom on the phenyl ring of Compound 1 is 3.49 from the backbone carbonyl oxygen of Pro154. Typically, to be classified as a halogen bond the distance between the donor and acceptor atoms must be equal to or less than the sum of the respective van der Waals radii which is 3.27Å for a Cl--O bond.[44,45] In their recent review Bissantz *et al.* list the typical interaction distance of a halogen bond (extracted from the crystal structure database) to be between 3–3.4 Å.[43] In our case the Cl--O bond distance of 3.49 Å leads us to believe that the influence of the Cl atom could be a combination of a halogen bond interaction as well as a good steric fit in the generally hydrophobic pocket. The results obtained when Cl is replaced with Br support this conclusion. The IC_{50} of 1-(4-bromobenzyl) benzimidazole is similar to 1-(4-chlorobenzyl) benzimidazole (27μM), as expected.[32] Substitution of the para-chlorine with fluorine, as in 1-(4-fluorobenzyl) benzimidazole results in a weaker inhibitor (IC_{50}>100μM), presumably due to the inherently smaller van der Waals radius and the inability of fluorine atoms to form halogen bonds.

Methyl substitutions on the benzimidazole group at positions 5 and 6 led to a further observed increase in activity. Interestingly, the position of the methyl groups on the benzimidazole scaffold fall at a position near the solvent exposed entrance to the enzyme's active site, which at first glance seems counterintuitive when considering the sharp increase in activity seen with this series.[32] Upon closer examination, however, the methyl substituents appear to be positioned near a hydrophobic surface formed by the residues Leu99, Met159, Ala196, Ile200, Ala94, and Phe93, which explains in part the preference for lipophilic substituents observed at this position. Inspection of the steric fit at this position reveals that there is considerable space that can accommodate larger substituents. The effect of the methyl group substituents on the general lipophilicity of the inhibitor compound as a potential explanation for the increase in activity must also be weighed, particularly considering the known preference of this enzyme for lipophilic compounds.

Lastly, substitution with a methyl at the 2-position on the benzimidazole group in 1-(3,4-dichlorobenzyl) benzimidazole group was well tolerated (IC_{50}=3.2μM) when compared to its parent compound 1-(3,4-dichlorobenzyl) benzimidazole (IC_{50}=4.7μM). However, substitution with an amino group at this position resulted in a complete loss of activity. Larger substitutions were also observed to result in a complete loss of activity (unpublished data). Now observable in the crystal structure, the 2-position is directed toward the carboxamide ring of NADH, facing the π-electron orbitals of the ring system. The obvious steric restraint at this position explains, in part, why only small substituents are tolerated. The increased activity of the methyl group over the amino substituent may be explained, as discussed above, by a general increase in lipophilicity of the inhibitor caused by methyl substitution versus amino substitution. We have theorized that electron donating groups at

this position would increase the strength of the hydrogen bond formed by the N_3 nitrogen, however the immediate reason for the methyl being favored over the amino, both of which can be considered electron donating, is not readily apparent.

Inhibition Kinetics Studies Confirm the Structural Observations Above

Many of the inhibitors based on the diphenyl ether scaffolds are known to be slow binding inhibitors that bind to the E-NAD^+ form of the enzyme more tightly than the E-NADH form.[10] Additionally, the crystal structures of the other inhibitor classes that have been published to date also suggest that these compounds bind to the E-NAD^+ form of the enzyme and form a key stacking interaction with the nicotinamide ring system as part of their binding mechanism. However, with the benzimidazole class of inhibitors, we were not able to grow crystals of the ternary complex (inhibitor-enzyme-cofactor) using NAD^+ in the crystallization buffer, but crystals readily grew when NADH was substituted. Crystals of the ternary complex with Compound 1 diffracted well but poor diffraction patterns were obtained with other benzimidazole analogs. Since crystals of benzimidazole compounds did not grow when only NAD^+ was present in the crystallization condition instead of NADH we hypothesized that the benzimidazole compounds do not bind in an uncompetitive manner with NAD^+ as is seen with other classes of inhibitors. To test this hypothesis, we investigated the pattern of inhibition of Compound 1 with respect to NADH and NAD^+. Product inhibition by NAD^+ was observed (data not shown) as was previously reported by others[10] however we did not observe any difference in the inhibition pattern of Compound 1 when 200μM of NAD^+ was present in the reaction mixture along with NADH. This further supports our hypothesis that the benzimidazole compounds preferentially bind to the E-NADH form of the enzyme over the E-NAD^+ form.

The K_m of NADH was found to 26.8 μM which is similar to that reported previously (18.8 μM).[10] We did not do a rigorous determination of the K_m of our substrate crotonyl-CoA due to its high cost and limited availability. However our preliminary experiments indicate the K_m to be ~830 μM. The K_i for Compound 1 was determined by varying the concentrations of the substrate at a fixed concentration (saturation concentration) of NADH (200μM). The experimental data were fit to the eqs 1–4 (Methods section) by nonlinear regression analysis (SigmaPlot with Enzyme Kinetics Module). The goodness of fit was evaluated on the basis of standard errors of the parameter estimates and the Akaike Information Criterion corrected for small sample size (AICc). The lowest AICc value in combination with some graphic analysis of experimental data was used for selection of the best model. Compound 1 was found to be competitive with respect to the substrate with the inhibition constant (K_i) being 0.36 μM (Figure 7). This inhibitor thus occupies the same area in the active site as does the substrate. We speculate that the carbonyl group of the substrate (Figure 1G) makes the very same hydrogen bond interactions with NADH and Tyr156 as does the benzimidazole N_3 atom in Compound 1. These interactions hold the substrate in place for catalysis to occur. The mechanism of inhibition of Compound 1 with respect to NADH was also determined in a similar fashion using different concentrations of NADH (6.25–200μM) at fixed sub-saturating concentration of substrate (500μM). Compound 1 displayed uncompetitive inhibition with respect to NADH as expected since NADH was bound to the enzyme with the inhibitor in the active site and makes a critical hydrogen bond with the inhibitor.

CONCLUSIONS

The benzimidazole series of compounds represent a novel inhibitor scaffold with very promising inhibition of FabI activity from both the Gram-negative *F. tularensis* as well as Gram-positive *B. anthracis*. We have presented here the solved co-crystal structure of a particularly active member of this class that reveals a binding mode in the active site of FabI that is unique compared to the binding patterns that have been reported for other classes of

FabI inhibitors to date. The solved structure explains the SAR of the series that had been previously reported and provides insight into further modification that will advance the series in further generations. Inhibition kinetics studies have confirmed that the inhibitor, and presumably the class, is uncompetitive with respect to the cofactor NADH and competitive with respect to the substrate. Addition of NAD^+ to the assay did not improve the activity of the compound. The crystallography, structure-activity relationship, and kinetic data, taken together, strongly suggest that the benzimidazole series preferentially bind to the enzyme-NADH complex over the enzyme-NAD^+ complex that other inhibitors favor. In addition to guiding future studies on this particular scaffold, we believe this new information regarding inhibitor binding may have a strong impact on the field in general.

Acknowledgments

This work was supported by National Institutes of Health Grant U01 AI077949. KEH was supported during a portion of this work by NIDCR 5T32-DE018381, UIC College of Dentistry, MOST Program. Data were collected at Southeast Regional Collaborative Access Team (SER-CAT) 22-IDbeamline at the Advanced Photon Source, Argonne National Laboratory. Use of the Advanced Photon Source was supported by the U. S. Department of Energy, Office of Science, Office of Basic Energy Sciences, under Contract No. DE-AC02-06CH11357. Marvin was used for drawing and displaying chemical structures, Marvin v5.9, 2012, ChemAxon, http://www.chemaxon.com. Figures were made using The PyMOL Molecular Graphics System, Version 1.0 Schrödinger, LLC.

Abbreviations

ACP	acyl-carrier protein
FAS	fatty acid synthase
NADH	nicotinamide adenine dinucleotide
NADPH	nicotinamide adenine dinucleotide phosphate
SDR	short-chain dehydrogenase/reductase

References

1. Boucher HW, Talbot GH, Bradley JS, Edwards JE, Gilbert D, Rice LB, Scheld M, Spellberg B, Bartlett J. Bad bugs, no drugs: no ESKAPE! An update from the Infectious Diseases Society of America. Clin Infect Dis. 2009; 48:1–12. [PubMed: 19035777]
2. Lu H, Tonge PJ. Inhibitors of FabI, an enzyme drug target in the bacterial fatty acid biosynthesis pathway. Acc Chem Res. 2008; 41:11–20. [PubMed: 18193820]
3. Bergler H, Fuchsbichler S, Hogenauer G, Turnowsky F. The enoyl-[acyl-carrier-protein] reductase (FabI) of Escherichia coli, which catalyzes a key regulatory step in fatty acid biosynthesis, accepts NADH and NADPH as cofactors and is inhibited by palmitoyl-CoA. Eur J Biochem. 1996; 242:689–694. [PubMed: 9022698]
4. White SW, Zheng J, Zhang YM, Rock. The structural biology of type II fatty acid biosynthesis. Annu Rev Biochem. 2005; 74:791–831. [PubMed: 15952903]
5. Miesel L, Greene J, Black TA. Genetic strategies for antibacterial drug discovery. Nature reviews. 2003; 4:442–456.
6. Heath RJ, Rock CO. A triclosan-resistant bacterial enzyme. Nature. 2000; 406:145–146. [PubMed: 10910344]
7. Heath RJ, Su N, Murphy CK, Rock CO. The enoyl-[acyl-carrier-protein] reductases FabI and FabL from Bacillus subtilis. J Biol Chem. 2000; 275:40128–40133. [PubMed: 11007778]
8. Massengo-Tiasse RP, Cronan JE. Vibrio cholerae FabV defines a new class of enoyl-acyl carrier protein reductase. J Biol Chem. 2008; 283:1308–1316. [PubMed: 18032386]

9. Marrakchi H, Dewolf WE Jr, Quinn C, West J, Polizzi BJ, So CY, Holmes DJ, Reed SL, Heath RJ, Payne DJ, Rock CO, Wallis NG. Characterization of Streptococcus pneumoniae enoyl-(acyl-carrier protein) reductase (FabK). Biochem J. 2003; 370:1055–1062. [PubMed: 12487627]
10. Lu H, England K, am Ende C, Truglio JJ, Luckner S, Reddy BG, Marlenee NL, Knudson SE, Knudson DL, Bowen RA, Kisker C, Slayden RA, Tonge PJ. Slow-onset inhibition of the FabI enoyl reductase from francisella tularensis: residence time and in vivo activity. ACS Chem Biol. 2009; 4:221–231. [PubMed: 19206187]
11. England K, am Ende C, Lu H, Sullivan TJ, Marlenee NL, Bowen RA, Knudson SE, Knudson DL, Tonge PJ, Slayden RA. Substituted diphenyl ethers as a broad-spectrum platform for the development of chemotherapeutics for the treatment of tularaemia. The Journal of antimicrobial chemotherapy. 2009; 64:1052–1061. [PubMed: 19734171]
12. Balemans W, Lounis N, Gilissen R, Guillemont J, Simmen K, Andries K, Koul A. Essentiality of FASII pathway for Staphylococcus aureus. Nature. 2010; 463:E3. discussion E4. [PubMed: 20090698]
13. Brinster S, Lamberet G, Staels B, Trieu-Cuot P, Gruss A, Poyart C. Type II fatty acid synthesis is not a suitable antibiotic target for Gram-positive pathogens. Nature. 2009; 458:83–86. [PubMed: 19262672]
14. Brinster S, Lamberet G, Staels B, Trieu-Cuot P, Gruss A, Poyart C. Brinster et al. reply. Nature. 2010; 463:E4–E5.
15. Parsons JB, Frank MW, Subramanian C, Saenkham P, Rock CO. Metabolic basis for the differential susceptibility of Gram-positive pathogens to fatty acid synthesis inhibitors. Proceedings of the National Academy of Sciences of the United States of America. 2011; 108:15378–15383. [PubMed: 21876172]
16. Raetz CR, Reynolds CM, Trent MS, Bishop RE. Lipid A modification systems in gram-negative bacteria. Annu Rev Biochem. 2007; 76:295–329. [PubMed: 17362200]
17. Oyston PC, Sjostedt A, Titball RW. Tularaemia: bioterrorism defence renews interest in Francisella tularensis. Nature reviews. 2004; 2:967–978.
18. Hepburn MJ, Simpson AJ. Tularemia: current diagnosis and treatment options. Expert Rev Anti Infect Ther. 2008; 6:231–240. [PubMed: 18380605]
19. Russell AD. Whither triclosan? The Journal of antimicrobial chemotherapy. 2004; 53:693–695. [PubMed: 15073159]
20. Yazdankhah SP, Scheie AA, Hoiby EA, Lunestad BT, Heir E, Fotland TO, Naterstad K, Kruse H. Triclosan and antimicrobial resistance in bacteria: an overview. Microbial drug resistance (Larchmont, NY. 2006; 2:83–90.
21. Moir DT. Identification of inhibitors of bacterial enoyl-acyl carrier protein reductase. Curr Drug Targets Infect Disord. 2005; 5:297–305. [PubMed: 16181147]
22. Chhibber M, Kumar G, Parasuraman P, Ramya TN, Surolia N, Surolia A. Novel diphenyl ethers: design, docking studies, synthesis and inhibition of enoyl ACP reductase of Plasmodium falciparum and Escherichia coli. Bioorganic & medicinal chemistry. 2006; 14:8086–8098. [PubMed: 16893651]
23. Freundlich JS, Anderson JW, Sarantakis D, Shieh HM, Yu M, Valderramos JC, Lucumi E, Kuo M, Jacobs WR Jr, Fidock DA, Schiehser GA, Jacobus DP, Sacchettini JC. Synthesis biological activity and X-ray crystal structural analysis of diaryl ether inhibitors of malarial enoyl acyl carrier protein reductase. Part 1: 4'-substituted triclosan derivatives. Bioorganic & medicinal chemistry letters. 2005; 15:5247–5252. [PubMed: 16198563]
24. Freundlich JS, Yu M, Lucumi E, Kuo M, Tsai HC, Valderramos JC, Karagyozov L, Jacobs WR Jr, Schiehser GA, Fidock DA, Jacobus DP, Sacchettini JC. Synthesis, biological activity of diaryl ether inhibitors of malarial enoyl acyl carrier protein reductase. Part 2: 2'-substituted triclosan derivatives. Bioorganic & medicinal chemistry letters. 2006; 16:2163–2169. [PubMed: 16466916]
25. Rafi SB, Cui G, Song K, Cheng X, Tonge PJ, Simmerling C. Insight through molecular mechanics Poisson-Boltzmann surface area calculations into the binding affinity of triclosan and three analogues for FabI, the E. coli enoyl reductase. Journal of medicinal chemistry. 2006; 49:4574–4580. [PubMed: 16854062]

26. Sivaraman S, Sullivan TJ, Johnson F, Novichenok P, Cui G, Simmerling C, Tonge PJ. Inhibition of the bacterial enoyl reductase FabI by triclosan: a structure-reactivity analysis of FabI inhibition by triclosan analogues. Journal of medicinal chemistry. 2004; 47:509–518. [PubMed: 14736233]
27. Tipparaju SK, Mulhearn DC, Klein GM, Chen Y, Tapadar S, Bishop MH, Yang S, Chen J, Ghassemi M, Santarsiero BD, Cook JL, Johlfs M, Mesecar AD, Johnson ME, Kozikowski AP. Design and synthesis of aryl ether inhibitors of the Bacillus anthracis enoyl-ACP reductase. ChemMedChem. 2008; 3:1250–1268. [PubMed: 18663709]
28. Grassberger MA, Turnowsky F, Hildebrandt J. Preparation and antibacterial activities of new 1,2,3-diazaborine derivatives and analogues. J Med Chem. 1984; 27:947–953. [PubMed: 6379179]
29. Seefeld MA, Miller WH, Newlander KA, Burgess WJ, DeWolf WE Jr, Elkins PA, Head MS, Jakas DR, Janson CA, Keller PM, Manley PJ, Moore TD, Payne DJ, Pearson S, Polizzi BJ, Qiu X, Rittenhouse SF, Uzinskas IN, Wallis NG, Huffman WF. Indole naphthyridinones as inhibitors of bacterial enoyl-ACP reductases FabI and FabK. Journal of medicinal chemistry. 2003; 46:1627–1635. [PubMed: 12699381]
30. Ling LL, Xian J, Ali S, Geng B, Fan J, Mills DM, Arvanites AC, Orgueira H, Ashwell MA, Carmel G, Xiang Y, Moir DT. Identification and characterization of inhibitors of bacterial enoyl-acyl carrier protein reductase. Antimicrob Agents Chemother. 2004; 48:1541–1547. [PubMed: 15105103]
31. Kitagawa H, Kumura K, Takahata S, Iida M, Atsumi K. 4-Pyridone derivatives as new inhibitors of bacterial enoyl-ACP reductase FabI. Bioorganic & medicinal chemistry. 2007; 15:1106–1116. [PubMed: 17095231]
32. Hevener KE, Mehboob S, Su PC, Truong K, Boci T, Deng J, Ghassemi M, Cook JL, Johnson ME. Discovery of a Novel and Potent Class of F. tularensis Enoyl-Reductase (FabI) Inhibitors by Molecular Shape and Electrostatic Matching. Journal of medicinal chemistry. 2012; 55:268–279. [PubMed: 22098466]
33. Kabsch WJ. XDS Appl Cryst. 1993:795–800.
34. McCoy AJ, Grosse-Kunstleve RW, Adams PD, Winn MD, Storoni LC, Read RJ. Phaser crystallographic software. Journal of applied crystallography. 2007; 40:658–674. [PubMed: 19461840]
35. Mehboob S, Truong K, Santarsiero BD, Johnson ME. Crystal Structure of the Francisella tularensis enoyl-acyl carrier protein reductase (FabI) in complex with NAD(+) and triclosan. Acta crystallographica. 2010; 66:1436–1440. [PubMed: 21045289]
36. Vagin AA, Steiner RA, Lebedev AA, Potterton L, McNicholas S, Long F, Murshudov GN. REFMAC5 dictionary: organization of prior chemical knowledge and guidelines for its use. Acta Crystallogr D Biol Crystallogr. 2004; 60:2184–2195. [PubMed: 15572771]
37. Emsley P, Lohkamp B, Scott WG, Cowtan K. Features and development of Coot. Acta Crystallogr D Biol Crystallogr. 2010; 66:486–501. [PubMed: 20383002]
38. Davis IW, Leaver-Fay A, Chen VB, Block JN, Kapral GJ, Wang X, Murray LW, Arendall WB 3rd, Snoeyink J, Richardson JS, Richardson DC. MolProbity: all-atom contacts and structure validation for proteins and nucleic acids. Nucleic Acids Res. 2007; 35:W375–383. [PubMed: 17452350]
39. Rafi S, Novichenok P, Kolappan S, Zhang X, Stratton CF, Rawat R, Kisker C, Simmerling C, Tonge PJ. Structure of acyl carrier protein bound to FabI, the FASII enoyl reductase from Escherichia coli. J Biol Chem. 2006; 281:39285–39293. [PubMed: 17012233]
40. Miller WH, Seefeld MA, Newlander KA, Uzinskas IN, Burgess WJ, Heerding DA, Yuan CC, Head MS, Payne DJ, Rittenhouse SF, Moore TD, Pearson SC, Berry V, DeWolf WE Jr, Keller PM, Polizzi BJ, Qiu X, Janson CA, Huffman WF. Discovery of aminopyridine-based inhibitors of bacterial enoyl-ACP reductase (FabI). Journal of medicinal chemistry. 2002; 45:3246–3256. [PubMed: 12109908]
41. He X, Alian A, Stroud R, Ortiz de Montellano PR. Pyrrolidine carboxamides as a novel class of inhibitors of enoyl acyl carrier protein reductase from Mycobacterium tuberculosis. Journal of medicinal chemistry. 2006; 49:6308–6323. [PubMed: 17034137]
42. Stewart MJ, Parikh S, Xiao G, Tonge PJ, Kisker C. Structural basis and mechanism of enoyl reductase inhibition by triclosan. J Mol Biol. 1999; 290:859–865. [PubMed: 10398587]

43. Bissantz C, Kuhn B, Stahl M. A medicinal chemist's guide to molecular interactions. J Med Chem. 2010; 53:5061–5084. [PubMed: 20345171]
44. Hernandes MZ, Cavalcanti SM, Moreira DR, de Azevedo Junior WF, Leite AC. Halogen atoms in the modern medicinal chemistry: hints for the drug design. Curr Drug Targets. 2010; 11:303–314. [PubMed: 20210755]
45. Lu Y, Shi T, Wang Y, Yang H, Yan X, Luo X, Jiang H, Zhu W. Halogen bonding--a novel interaction for rational drug design? J Med Chem. 2009; 52:2854–2862. [PubMed: 19358610]
46. Baldock C, Rafferty JB, Sedelnikova SE, Baker PJ, Stuitje AR, Slabas AR, Hawkes TR, Rice DW. A mechanism of drug action revealed by structural studies of enoyl reductase. Science. 1996; 274:2107–2110. [PubMed: 8953047]
47. Heerding DA, Chan G, DeWolf WE, Fosberry AP, Janson CA, Jaworski DD, McManus E, Miller WH, Moore TD, Payne DJ, Qiu X, Rittenhouse SF, Slater-Radosti C, Smith W, Takata DT, Vaidya KS, Yuan CC, Huffman WF. 1,4-Disubstituted imidazoles are potential antibacterial agents functioning as inhibitors of enoyl acyl carrier protein reductase (FabI). Bioorganic & medicinal chemistry letters. 2001; 11:2061–2065. [PubMed: 11514139]

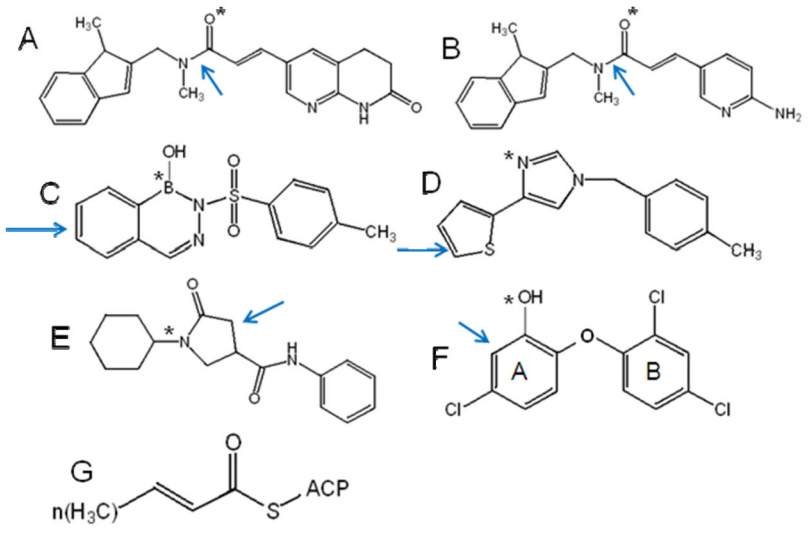

Figure 1.

Structures of known FabI inhibitors with the key binding features highlighted. (A) Indole naphthyridinones,[29] (B) aminopyridines,[29] (C) Diazaborines,[46] (D) disubstituted imidazoles,[47] (E) pyrrolidine carboxamide,[41] and (F) triclosan.[35] The arrows points to the aromatic or delocalized planar moiety that participates in π-stacking interactions with the NAD^+ cofactor. The * indicates the hydrogen bond accepting group that can interact with the 2'-hydroxyl group in the ribose ring of NAD^+ cofactor. (G) Structure of Trans-2-enoyl-ACP, the natural substrate of FabI. In our assays we use crotonyl-CoA as the substrate of FabI where coenzyme A is substituted for ACP.

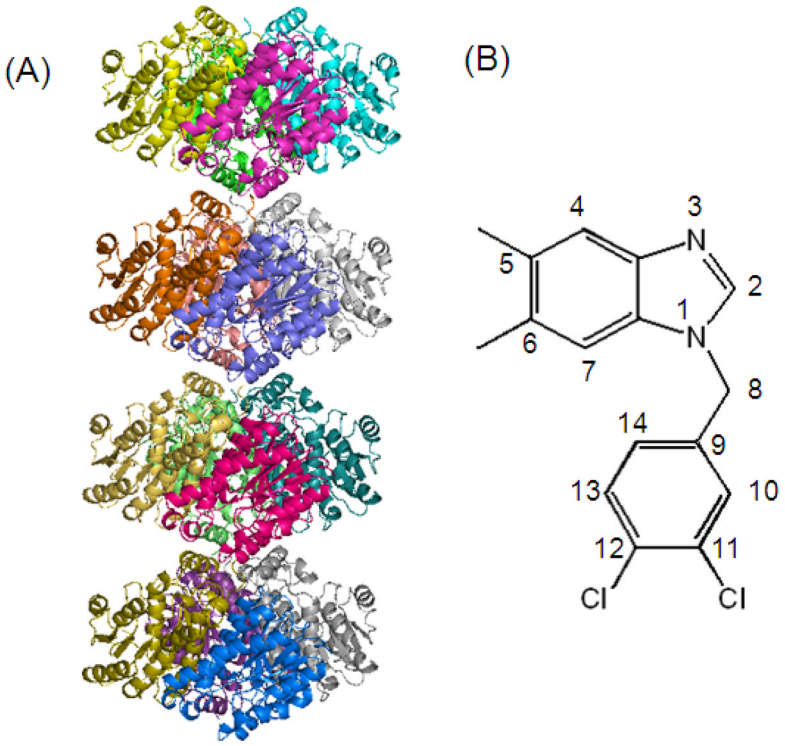

Figure 2.
(A) The crystal structure of FtuFabI in complex with Compound 1 contains 16 chains in the asymmetric unit with 4 tetramers stacked up on one another. (B) Structure of Compound 1.

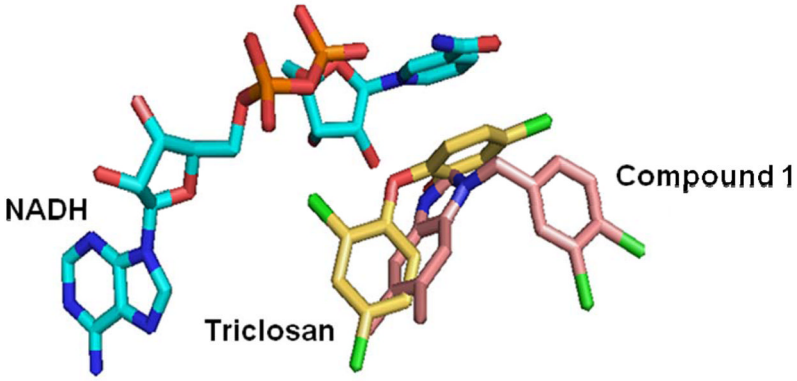

Figure 3.
Orientation of NADH, Triclosan and Compound 1 in the active site of FtuFabI. The enzyme has been omitted for clarity purposes. Triclosan and Compound 1 occupy similar space in the active site however unlike triclosan the π-stacking interaction of the benzimidazole ring or the phenyl ring of Compound 1 against nicotinamide ring of NADH is not observed.

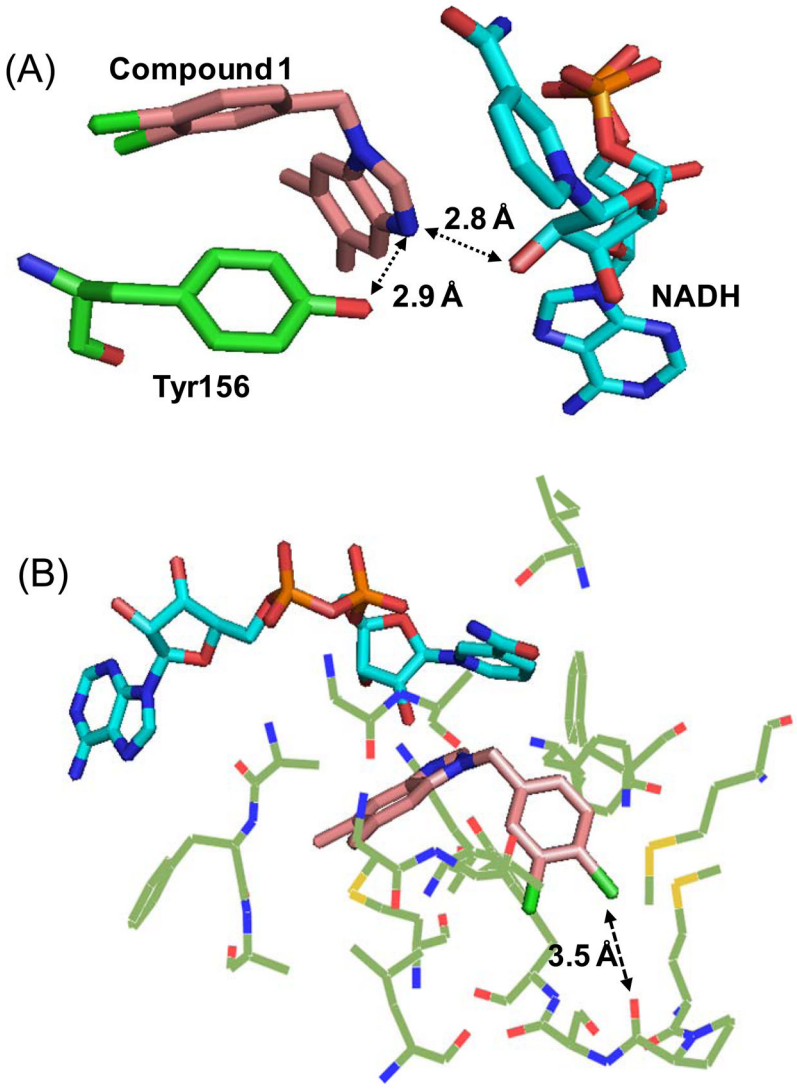

Figure 4.

Positioning of Compound 1 in the active site of FtuFabI. (A) The N_3 atom of the benzimidazole ring system of Compound 1 is within hydrogen bonding distance from the 2'-hydroxyl group of NADH and the hydroxyl group of Tyr156. (B) The para-chloro atom is positioned 3.5 away from the carbonyl group of Pro154, and the methylene linker is directed towards the amide group of the nicotinamide ring in NADH.

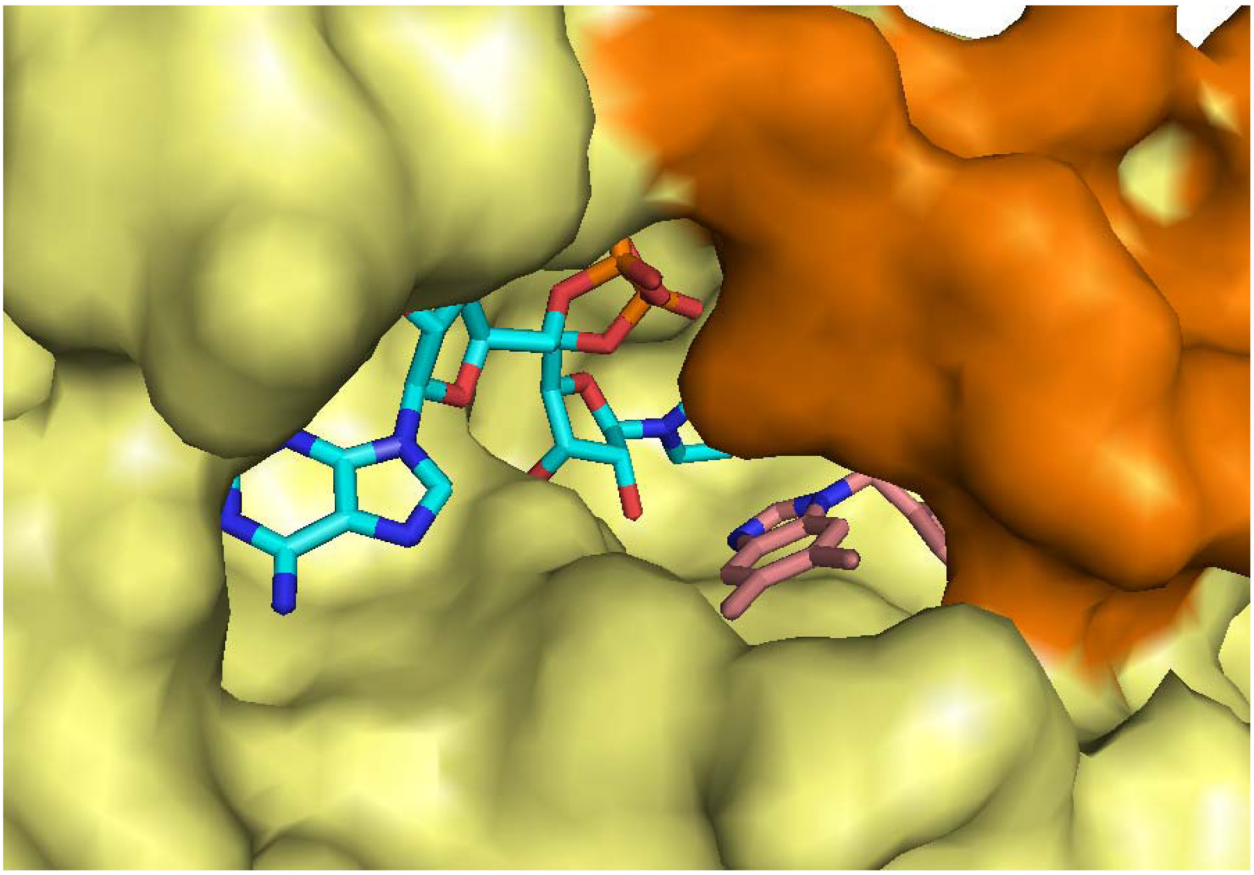

Figure 5.
Active site pocket Compound 1 (salmon) and NADH (cyan) in the active site of FtuFabI. The loop region (residues 190–203 colored orange) adopts a closed conformation in this structure forming critical interactions with the inhibitor and NADH.

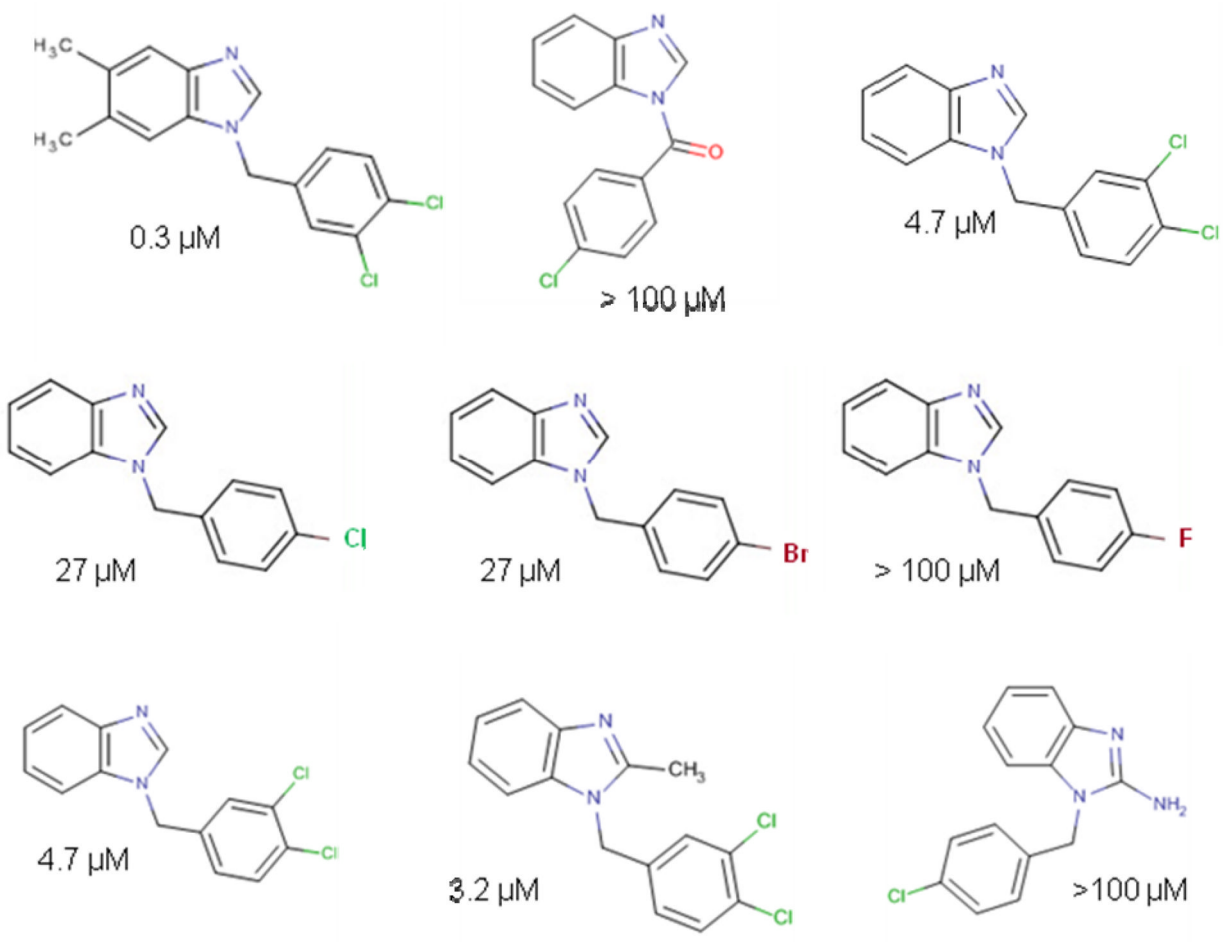

Figure 6.
IC_{50} values of several analogs of Compound 1[32] discussed in the text.

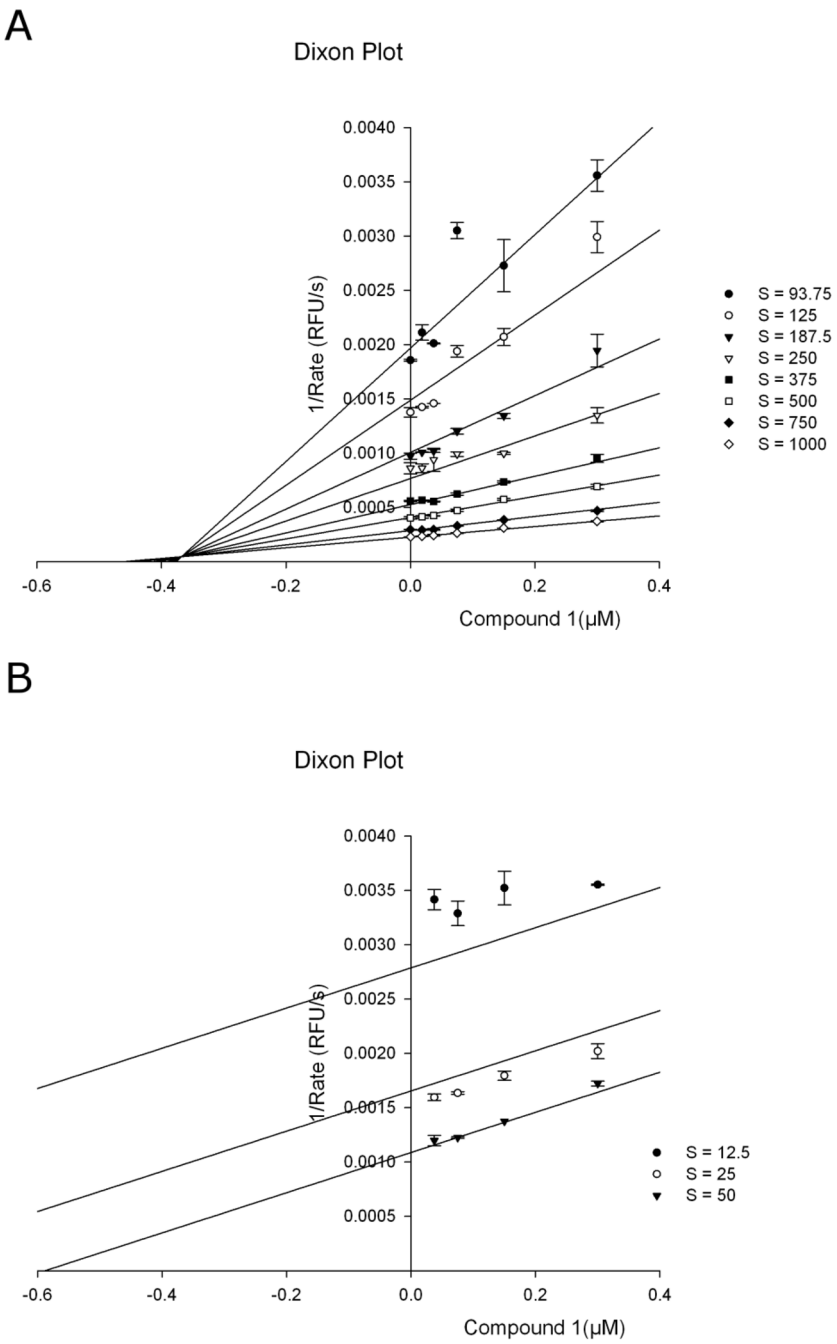

Figure 7.

(A) Dixon plot for competitive inhibition of Compound 1 with respect to the substrate crotonyl-CoA. The K_i was determined to be 0.36μM. (B) Dixon plot for uncompetitive inhibition of Compound 1 with respect to NADH (S=NADH). The experimental data used to generate these plots were fit by nonlinear regression analysis (in SigmaPlot with Enzyme Kinetics Module1.3) to equations 1–4 (Methods section) and represent a global fit of the data for all concentrations. Each of the two plots represents the best fit to the most appropriate kinetic model

Table 1

Data Collection and Refinement Statistics. Statistics for highest resolution shell are given in parentheses.

Data Collection	
Space group	P 2_1
Unit cell parameters:	
a,b,c (Å)	*a* = 85.41, *b* = 123.46 *c* = 203.33
Resolution (Å)	2.3 (2.40–2.26)
No. reflections	1122813 (88235)
No. averaged reflections (unique)	356995 (39737)
R_{merge} (%)	10.7 (53.0)
I/σI	9.4 (2.1)
Completeness %	91.8 (63.4)
Refinement	
Resolution range (Å)	20.0 – 2.5
no. reflections in working set	137932
no. reflections in test set	7281
R_{crys} (%)	24.1
R_{free} (%)	29.2
Wilson B ($Å^2$)	29.8
average B-factor ($Å^2$) (protein)	30.6
No. of protein molecules in asymmetric unit	16
RMSD from ideal geometry:	
Bond lengths (Å)	0.016
Bond angles (deg)	1.816
Ramachandran plot	
allowed (%)	95.1
generous (%)	0.4
disallowed (%)	0.00